Volume 22
Number 12
June 8, 1983

Inorganic Chemistry

Contribution from the Department of Chemistry, University of Cincinnati, Cincinnati, Ohio 45221,
and the Miami Valley Laboratories, Procter & Gamble Company, Cincinnati, Ohio 45239

Synthesis, Characterization, and Electrochemical Properties of Tertiary Diphosphine Complexes of Technetium: Single-Crystal Structure of the Prototype Complex *trans*-$[Tc(DPPE)_2Br_2]BF_4$[1]

KAREN LIBSON,[2] B. L. BARNETT,[3] and EDWARD DEUTSCH*[2]

Received October 12, 1982

A series of nine Tc(III)/Tc(II) pairs of complexes having the formula *trans*-$[TcD_2X_2]^{+/0}$, where D represents a chelating tertiary diphosphine ligand and X represents Cl, Br, or SCN, has been synthesized and characterized. This series includes the five diphosphine ligands 1,2-bis(diphenylphosphino)ethane (DPPE), *cis*-bis(1,2-diphenylphosphino)ethylene (DPPV), bis(1,2-diphenylphosphino)benzene (DPPB), bis(1,2-dimethylphosphino)ethane (DMPE), and bis(1,2-diethylphosphino)ethane (DEPE). There are several preparative routes to these complexes, the most practical involving reduction of higher oxidation states of technetium by excess diphosphine and concomitant ligand substitution onto the reduced technetium center. The prototype title complex, $\{Tc[(C_6H_5)_2PCH_2CH_2P(C_6H_5)_2]_2Br_2\}BF_4$, formula weight 1142.46, has been characterized by single-crystal X-ray structural analysis refined to a conventional R factor of 0.046. Hexagonal red crystals of this moiety crystallize in the trigonal space group $P\bar{3}$ with a = 20.926 (5) Å, c = 11.178 (2) Å, and Z = 3. In this complex the technetium(III) center is approximately octahedrally coordinated with four equatorial P atoms at an average distance of 2.50 (2) Å and two trans axial Br atoms at 2.440 (1) Å. Other complexes in the series have been characterized by some combination of elemental analysis, IR and vis-UV spectrophotometry, thin-layer and high-performance liquid chromatography, magnetic measurements, and cyclic voltammetry (CV). All complexes exhibit a characteristic, intense halogen-to-technetium charge-transfer (HTTCT) band in the visible region of the spectrum. The energy of this HTTCT transition is a function of the oxidation state of the technetium, the nature of the halogen (or pseudohalogen) ligands, X, and the nature of the substituents bonded to the donor phosphorus atoms. CV shows that in *N,N*-dimethylformamide, with use of gold, platinum, or glassy carbon electrodes, every complex in the series exhibits a reversible Tc(III)/Tc(II) redox couple. The $E^{\circ\prime}$ of this Tc(III)/Tc(II) couple depends on the nature of the coordinated halogen (or pseudohalogen) ligands and on the nature of the substituents bonded to the donor phosphorus atoms. For closely related systems, the $E^{\circ\prime}$ of the Tc(III)/Tc(II) couple is linearly related to the energy of the HTTCT transition. All complexes exhibit a Tc(II)/Tc(I) cathodic wave, but only for $[Tc(DPPE)_2(SCN)_2]^{0/-}$, $[Tc(DMPE)_2Cl_2]^{0/-}$, and $[Tc(DMPE)_2Br_2]^{0/-}$ is this couple reversible. Under the specified experimental conditions, none of the complexes exhibit any evidence for either a reversible or an irreversible Tc(IV)/Tc(III) couple.

Introduction

Research into the preparation and chemistry of technetium complexes has increased markedly during the last several years.[4-10] Much of this activity arises from the utility of technetium complexes in diagnostic nuclear medicine wherein different chemical forms of technetium-99m are used to image a wide variety of organs.[4-10] The vast majority of technetium complexes so employed have been *anionic*. Typical of these negatively charged complexes are pertechnetate (TcO_4^-), used to detect defects in the blood brain barrier, and the technetium diphosphonate agents used to image bone.[11,12] There has recently developed an interest in *cationic* technetium complexes, and this interest also derives much of its impetus from the requirements of nuclear medicine.[13] The propensity of the heart to accumulate unit positively charged metal ions is well documented,[10] and thallium-201 as $[Tl(aq)]^+$ is the heart-scanning agent currently used in hospitals around the country. For the past several years we have been interested in the development of robust *cationic* technetium complexes for potential use as myocardial imaging agents.[10] In the course of this work some monomeric, positively charged, technetium

---

(1) Abstracted in part from the Ph.D. thesis of K.L., University of Cincinnati, 1981.
(2) University of Cincinnati.
(3) Procter & Gamble Co.
(4) Deutsch, E.; Libson, K.; Jurisson, S.; Lindoy, L. F. *Prog. Inorg. Chem.* **1983**, *30*, 75.
(5) Bandoli, G.; Mazzi, U.; Roncari, E.; Deutsch, E. *Coord. Chem. Rev.* **1982**, *44*, 191.
(6) Deutsch, E.; Barnett, B. L. In "Inorganic Chemistry in Biology and Medicine"; Martell, A. E., Ed.; American Chemical Society: Washington, DC, 1980; ACS Symp. Ser. No. 140, pp 103-119.
(7) Deutsch, E. In "Radiopharmaceuticals II", Proceedings of the 2nd International Symposium on Radiopharmaceuticals; Society of Nuclear Medicine: New York, 1979; pp 129-146.
(8) Siegel, J. A.; Deutsch, E. *Annu. Rep. Inorg. Gen. Synth.* **1976**, 311-326.
(9) Clark, M. J.; Fackler, P. H. *Struct. Bonding (Berlin)* **1982**, *50*, 57-78.
(10) Deutsch, E.; Glavan, K. A.; Bushong, W.; Sodd, V. J. In "Applications of Nuclear Chemistry and Radiochemistry"; Lambrecht, R., Marcos, N., Eds.; Pergamon Press: New York, 1982; 139-151.
(11) Saha, G. B. "Fundamentals of Nuclear Pharmacy"; Springer-Verlag: New York, 1979; pp 187-192.
(12) Francis, M. D.; Ferguson, D. L.; Tofe, A. J.; et al. *J. Nucl. Med.* **1980**, *23*, 1185-1189.
(13) Deutsch, E.; Bushong, W.; Glavan, K. A.; Elder, R. C.; Sodd, V. J.; Scholz, K. L.; Fortman, D. L.; Lukes, S. J. *Science* **1981**, *214*, 85.

0020-1669/83/1322-1695$01.50/0 © 1983 American Chemical Society

complexes were synthesized, characterized, and subsequently tested for accumulation in myocardial tissue. The heart of a mongrel dog was successfully imaged by using complexes of the general formula *trans*-$[^{99m}TcD_2X_2]^+$, where D represents a chelating tertiary diarsine or diphosphine ligand and X represents a halogen.

As a class, both the tertiary diarsine and diphosphine ligands have proven capable of stabilizing transition metals in a variety of unusual oxidation states and coordination geometries, and these ligands have been widely used in coordination chemistry for the past two decades.[14,15] Fergusson and Nyholm[16] were the first to prepare technetium complexes of *o*-phenylenebis(dimethylarsine) (DIARS), and later Fergusson reported the preparation of some Tc and Re complexes of 1,2-bis(diphenylphosphino)ethane (DPPE).[17] In this paper we report the synthesis, characterization, and electrochemical properties of a series of cationic technetium-99 complexes of tertiary diphosphine ligands that are related to DPPE and present the single-crystal structure analysis of the prototype cationic complex *trans*-$[^{99}Tc(DPPE)_2Br_2]^+$ as the BF_4^- salt.

Acronyms and Abbreviations

Compounds: TDP = tertiary diphosphine; DPPE = 1,2-bis(diphenylphosphino)ethane; DPPV = *cis*-bis(1,2-diphenylphosphino)ethylene; DPPB = bis(1,2-diphenylphosphino)benzene; DEPE = bis(1,2-diethylphosphino)ethane; DMPE = bis(1,2-dimethylphosphino)ethane; DIARS = *o*-phenylenebis(dimethylarsine); tu = thiourea; TEAP = tetraethylammonium perchlorate.

Solvents: Me_2SO = dimethyl sulfoxide; DMF = *N,N*-dimethylformamide; THF = tetrahydrofuran.

Techniques: HPLC = high-performance liquid chromatography; TLC = thin-layer chromotography; CV = cyclic voltammetry.

Miscellaneous: LTMCT = ligand-to-metal charge transfer; HTTCT = halogen-to-technetium charge transfer.

Experimental Section

General Information. Technetium-99 emits a low-energy (0.292 MeV) β particle with a half-life of 2.12×10^5 years. When this material is handled in milligram amounts, it does not present a serious health hazard since common laboratory materials provide adequate shielding. Bremsstrahlung is not a significant problem due to the low energy of the β-particle emission, but normal radiation safety procedures must be used at all times to prevent contamination.

Reactions involving phenyl-substituted TDP ligands were conducted in the presence of air with use of solvents that were not deoxygenated. The alkyl-substituted TDP ligands were stored under an inert atmosphere, and reactions were conducted with use of deoxygenated solvents under a blanket of either argon or carbon dioxide. Elemental analyses were performed by Galbraith Laboratories, Knoxville, TN, or by Guelph Chemical Laboratories Ltd., Guelph, Ontario, Canada.

Methods. Unless otherwise noted, all chemicals were of reagent grade. All TDP ligands were purchased from Strem Chemical Co. and used without further purification. Technetium-99, in the form of solid ammonium pertechnetate ($NH_4{}^{99}TcO_4$), was purchased from Oak Ridge National Laboratory and purified as outlined below. The ammonium hexahalotechnetate(IV) complexes (X = Cl, Br, I) were synthesized according to a literature procedure[18] and converted to the less soluble potassium and tetrabutylammonium salts by simple metathesis in aqueous media. Tetrabutylammonium tetrachlorooxotechnetate(V) was prepared by the method of Davison,[19] as was hexakis(thiourea)technetium(III) chloride.[20] *N,N*-Dimethylformamide (DMF, Omnisolv, MCB) and tetraethylammonium perchlorate (TEAP, G. F. Smith), labeled respectively "suitable for spectrophotometry" and "suitable for polarography", were used in the electrochemical experiments.

Table I. Elemental Analyses for Selected Technetium(III) and Technetium(II) Complexes of Tertiary Diphosphine Ligands

complex		% C	% H	% P	% X[a]	% S
$[Tc(DPPE)_2Cl_2]Cl$	calcd	62.32	4.82		10.61	
	exptl	60.94	5.02		10.75	
$[Tc(DMPE)_2Cl_2]$-SO_3CF_3	calcd	25.2	5.18	20.01	11.45	5.18
	exptl	25.86	5.03	19.92	11.90	5.30
$[Tc(DMPE)_2Br_2]$-SO_3CF_3	calcd	22.05	4.55	17.49	22.57	
	exptl	22.09	4.16	17.61	23.88	
$[Tc(DPPB)_2Cl_2]Cl$	calcd	65.60	4.40	11.28	9.68	
	exptl	62.58	5.36	9.26	10.54	
$Tc(DPPE)_2(SCN)_2\cdot{}^1/_2CH_2Cl_2$	calcd	62.07	4.68	11.75	3.36	6.08
	exptl	61.03	4.79	11.87	3.71	5.72

[a] X = Cl, Br.

Table II. Visible-UV Spectrophotometric Parameters for Technetium(III) and Technetium(II) Complexes of Tertiary Diphosphines

compd	solvent	color	λ_{max}, nm (ϵ, M^{-1} cm^{-1})
$Tc^{II}(DPPE)_2(SCN)_2{}^0$	CH_2Cl_2	violet	534
$Tc^{II}(DPPE)_2Cl_2{}^0$	CH_2Cl_2	yellow	420
$Tc^{II}(DPPB)_2Br_2{}^0$	pyridine	yellow	470 (4980), 421 (1610)
$Tc^{II}(DPPB)_2Cl_2{}^0$	pyridine	yellow	438
$Tc^{II}(DPPV)_2Br_2{}^0$	toluene	yellow	461
$Tc^{II}(DPPV)_2Cl_2{}^0$	toluene	yellow	424
$Tc^{II}(DEPE)_2Cl_2{}^0$	DMF	yellow	410
$Tc^{II}(DMPE)_2Cl_2{}^0$	DMF	yellow	414
$Tc^{II}(DEPE)_2Br_2{}^0$	toluene	green	438 (4410), 392 (317), 313 (2980)
$Tc^{II}(DMPE)_2Br_2{}^0$	CH_2Cl_2	green	439
$Tc^{III}(DPPE)_2(SCN)_2{}^+$	CH_2Cl_2	blue	584
$Tc^{III}(DPPE)_2Br_2{}^+$	ethanol	dark pink	504 (4200)
$Tc^{III}(DPPE)_2Cl_2{}^+$	ethanol	orange-red	480 (2500)
$Tc^{III}(DPPB)_2Cl_2{}^+$	ethanol	red	492
$Tc^{III}(DPPV)_2Cl_2{}^+$	ethanol	orange-red	475
$Tc^{III}(DEPE)_2Br_2{}^+$	ethanol	rose red	493 (5040), 330 (3392), 268 (5639)
$Tc^{III}(DEPE)_2Cl_2{}^+$	ethanol	orange	464, 388 (sh)
$Tc^{III}(DMPE)_2Br_2{}^+$	ethanol	red	497, 325
$Tc^{III}(DMPE)_2Cl_2{}^+$	ethanol	orange	463

Ammonium Pertechnetate, NH_4TcO_4. The solid ammonium pertechnetate purchased from Oak Ridge National Laboratory was contaminated with technetium dioxide $(TcO_2)_n$. When necessary, the following procedure was used to provide pure material. NH_4TcO_4 was dissolved in H_2O with heating and stirring. A resulting dark gray cloudy solution indicated the presence of suspended technetium dioxide, which was then either (a) oxidized to TcO_4^- with excess 30% H_2O_2 or (b) mechanically separated from the solution by centrifugation. Recrystallization was from either hot H_2O or H_2O/ethanol. Metathesis to less soluble salts (e.g., K^+ or $N(CH_3)_4{}^+$) was effected by the addition of the appropriate chloride (e.g., KCl or $(CH_3)_4NCl$) to an almost saturated solution of NH_4TcO_4. Metathesis to a salt more soluble than NH_4TcO_4 required the use of a cation exchanger to convert NH_4TcO_4 to $HTcO_4$, followed by the addition of a salt of the desired cation.

Dihalogenobis(tertiary diphosphine)technetium(II) Complexes, $Tc^{II}D_2X_2{}^0$ (D = DPPE, DPPB, DPPV, DEPE; X = Cl, Br). For the three air-stable, phenyl-substituted ligands, tetrabutylammonium hexahalotechnetate and at least a 10-fold excess of ligand were

---

(14) McAuliffe, C. A. "Transition Metal Complexes of Phosphorus, Arsenic and Antimony Ligands"; Wiley: New York, Toronto, 1973.

(15) McAuliffe, C. A.; Levason, W. "Phosphine, Arsine and Stibine Complexes of the Transition Elements"; Elsevier: Amsterdam, Oxford, New York, 1979.

(16) Fergusson, J. E.; Nyholm, R. S. *Chem. Ind. (London)* **1960**, 347–348.

(17) Fergusson, J. E.; Hickford, J. H. *Aust. J. Chem.* **1970**, *23*, 453.

(18) Dalziel, J.; Gill, N. S.; Nyholm, R. S.; Peacock, R. D. *J. Chem. Soc.* **1958**, 4012.

(19) Davison, A.; Trop, H. S.; Sohn, M.; DePamphilis, B. V.; Jones, A. G. *Inorg. Synth.* **1982**, *21*, 160.

(20) Jones, A. G.; Davison, A. *Int. J. Appl. Radiat. Isot.* **1982**, *33*, 867.

dissolved in hot DMF and the reaction mixture was then stirred at 100–110 °C for several (3–8) hours. A typical preparation employing DPPE and $(Bu_4N)_2TcCl_6$ involves 1.2 of g DPPE $(3.0 \times 10^{-3}$ mol) and 0.2 g of $(Bu_4N)_2TcCl_6$ $(2.9 \times 10^{-4}$ mol) in a total of 25 mL of DMF. The yellow Tc(II) product is not very soluble in DMF and precipitates upon formation. The $TcD_2Cl_2^0$ complexes can be crystallized from either heptane/CH_2Cl_2 or toluene/ethanol. Yields were usually greater than 75%. Analytical and spectrophotometric data are given in Tables I and II. The $TcD_2Br_2^0$ complexes are susceptible to oxidation and are therefore not readily purified by crystallization. A typical preparation involving DEPE and $(Bu_4N)_2TcBr_6$ involves bringing the air–sensitive DEPE ligand into reaction with the hexabromotechnetate(IV) salt (ligand to metal ratio = 24) under a blanket of argon in 20 mL of hot (100 °C) DMF. Fine green needles of $Tc(DEPE)_2Br_2^0$ formed in approximately 15 min. These were filtered, washed successively with absolute ethanol and ether, and then dried in a vacuum desiccator for 2 h. The yield was 75%. Spectrophotometric data are given in Table II.

Dihalogenobis(tertiary diphosphine)technetium(III) Salts, $[TcD_2X_2]Y$ (D = DPPE, DPPB, DPPV, DEPE, DMPE; X = Cl, Br; Y = Cl, Br, ClO_4, NO_3, CF_3SO_3, SCN). Method 1. D = DPPE, DPPB, DPPV; X = Cl. Tetrabutylammonium hexachlorotechnetate was dissolved in hot, stirred DMF with a 10-fold excess of the desired ligand. The reaction mixture was periodically monitored via TLC and/or visible–UV spectrophotometry for the appearance of significant amounts of the desired Tc(III) product. The reaction usually required from 1 to 2 h to proceed to completion (depending upon variables such as temperature, concentration of reagents, and nature of TDP ligand). The mixture was cooled, excess ligand was removed by filtration, and the filtrate was diluted with toluene by at least 50-fold. In some cases a portion of the Tc(III) product precipitated at this point and could be removed by filtration. In most cases the bulk of the desired product remained in solution and was isolated by column chromatography. When D = DPPE, the toluene-diluted reaction mixture was loaded onto a column prepared by slurrying silica gel (activated, 100–200 mesh, Davison Chemical) in toluene. The cationic product adhered to the top of the column while excess ligand and any Tc(II) product were eluted during either the loading process or a subsequent toluene wash. The red Tc(III) product was then eluted in a tight band, with absolute ethanol. The product was isolated as a solid either by evaporation of the solvent or after precipitation by the addition of toluene or heptane. Purification was by crystallization from heptane/CH_2Cl_2 or toluene/ethanol. When D = DPPB or DPPV, the resulting Tc(III) products had low affinity for silica and were purified on alumina (Woelm, acid alumina, anionotropic, active grade 1) by using the above toluene/ethanol elution profile. When D = DEPE or DMPE, the reactions were conducted anaerobically in sealed reaction vials, either in hot DMF (100 °C) or in absolute ethanol (80–100 °C), with a ligand to metal ratio of greater than 20. Reaction times were less than those employed in the corresponding reactions with phenyl-substituted ligands, being on the order of 15 min to 1 h. Column chromatography on alumina, in conjunction with the toluene/ethanol elution profile noted above, could be used to separate the Tc(III) from the Tc(II) product, but the excess TDP ligand (presumably in an oxidized form) could not be removed by this procedure, and subsequent recrystallization of the product was necessary for complete purification. Yields ranged from 30 to 60%.

Method 2. D = DPPE, DPPB, DPPV, DEPE, DMPE; X = Cl, Br. A slurry of the appropriate technetium(II) $TcD_2Cl_2^0$ complex in toluene, chloroform, or CCl_4 was treated with Cl_2 gas for 5–15 min. The $[TcD_2Cl_2]Cl$ product precipitated upon formation. The analogous oxidation of $TcD_2Br_2^0$ by Br_2 was not always successful. Instead, $TcD_2Br_2^0$ was dissolved in toluene, a small amount of HBr was added, and filtered air was then bubbled through the mixture for 1–10 h (depending upon how amenable the particular complex was to air oxidation). The $[TcD_2Br_2]Br$ product precipitated upon formation. The addition of concentrated HNO_3 to a solution of $Tc(DPPE)_2Br_2^0$ in DMF resulted in the formation of $[Tc(DPPE)_2Br_2]NO_3$.

Method 3. D = DPPE; X = Cl. About 20–25 mg of ammonium pertechnetate was dissolved in DMF, which was approximately 0.1 M in ammonium chloride. A 50-fold excess of ligand was added, and the resulting mixture was heated and stirred until a color change to orange was effected (about 1 h). The reaction mixture was diluted with toluene and loaded onto a silica gel column prepared in toluene. The major orange product adhered to the top of the column while minor products and excess ligand washed through with toluene. This orange material was eluted with ethanol, and a visible–UV spectrum revealed the characteristic 480-nm peak of $[Tc(DPPE)_2Cl_2]^+$ (Table II).

Bis(thiocyanato)bis(1,2-bis(diphenylphosphino)ethane)technetium(II), $Tc(DPPE)_2(SCN)_2^0$. This material was prepared by the action of excess LiSCN on $[Tc(DPPE)_2X_2]^+$ (X = Cl, Br) in DMF or ethanol at 80–100 °C. After several hours, the color of the solution changed from either orange (dichloro complex) or red (dibromo complex) to purple, and the Tc(II) product precipitated from solution. Yields were in the range 30–50%. Analytical and spectrophotometric data are given in Tables I and II.

Halogen Exchange. A solution of $[Tc(DPPE)_2Cl_2]Cl$ (50 mg) and LiBr (40 mg) in 18 mL of 83% ethanol was refluxed for 6 h. The reaction mixture was periodically monitored (four times during the 6-h period) via visible–UV spectrophotometry. At the end of 6 h the following had occurred: (a) the characteristic HTTCT peak had shifted from 480 to 487 nm and (b) a small amount of red precipitate (3 mg) had formed. The visible–UV spectrum of this red material exhibited a maximum at 501 nm. The bulk of the technetium complexes were then precipitated by the addition of $LiPF_6$. The resulting $[Tc(DPPE)_2X_2]PF_6$ salt was redissolved in CH_2Cl_2, crystallized from CH_2Cl_2/toluene, and dried overnight in a vacuum desiccator. Elemental analysis of this material showed the presence of both Cl and Br in a ratio of 7 to 2. There was no indication of $Tc(DPPE)_2Br_2^0$ formation, contrary to the original report of Fergusson.[17]

Characterization. Most of the TDP–technetium complexes are characterized by at least five of the eight techniques employed in this study (X-ray diffraction, visible–UV and IR spectrophotometry, elemental analysis, TLC, HPLC, CV, and magnetic measurements). In the case of the $[Tc(DPPV)_2X_2]^{+/0}$ complex, characterization was by its visible–UV spectrum, by its TLC behavior, and by analogy to the chemistry and properties of the other complexes in this closely related series. The $[Tc(DPPV)_2Cl_2]^{+/0}$ Tc(III)/Tc(II) couple is not included in Table XI because the cyclic voltammograms of the chloride and tetrafluoroborate salts did not exhibit the same $E^{\circ\prime}$ value. For $[Tc(DPPV)_2Cl_2]Cl$ $E^{\circ\prime} = +150$ mV; for $[Tc(DPPV)_2Cl_2]BF_4$ $E^{\circ\prime} = +63$ mV. Both salts, however, exhibited the same visible–UV spectrophotometric parameters.

TLC experiments were conducted with use of cellulose, silica, or alumina flexible plastic-backed plates (Eastman Kodak) or glass-supported C_{18} plates (Whatman, MK C_{18}), all containaing a fluorescent indicator. Solvents were allowed to develop along at least 70% of a typically sized (3 × 8 cm) plate for determination of R_f values. Spots were measured from center to center except in cases where steaking and spreading were significant. In this latter situation the measurement was made from the center of the origin to the front of the spot. The phenyl-substituted diphosphines (as the free, oxidized, or coordinated ligand) were visualized with UV irradiation. The alkyl-substituted ligands (free or oxidized) were visualized in an iodine chamber. These latter species appeared as transient brown spots, which often decolorized upon exposure to air. Relevent R_f values are compiled in Table VII.

High-performance liquid chromatography (HPLC) experiments were conducted on a Beckman Model 302 dual-pump apparatus equipped with (1) a guard column containing Whatman CoPell ODS precolumn packing and (2) a Jones RPC-18 analytical column (250 × 4.5 mm). A Beckman Model 153 high-sensitivity analytical detector with a 254-nm filter insert was employed. The mobile phase consisted of a 50/30/20 mixture of methanol/tetrahydrofuran/X, where X is an aqueous solution containing 0.02 M sodium heptanesulfonate and 0.003 M phosphate buffer (pH 7.0). The flow rate was 1.5 mL/min and the pressure was usually between 2000 and 3000 psi. Relevant HPLC retention times are given in Table VII.

Physical Measurements. Electrochemical data were obtained with a Bioanalytical Systems Inc. CV-5 voltammograph apparatus and VC-2 cell with 0.5 M TEAP in DMF as the electrolytic medium. Cyclic voltammograms were obtained under anaerobic conditions vs. a Ag/AgCl reference electrode (filling solution 3.0 M NaCl; the potential of this electrode is −35 mV relative to SCE[21]) with use of gold, platinum, or glassy carbon working electrodes. The sweep rate varied from 5 to 500 mV s^{-1} with the average being 25 mV s^{-1}. At the beginning of every set of CV experiments, base lines were obtained

---

(21) Supplementary material from Bioanalytical Systems. CV notes: "The Silver/Silver Chloride Electrode"; Bioanalytical Systems: West Lafayette, IN.

by using the solvent, the supporting electrolyte, and, where appropriate, an inert chloride or bromide salt. It was found that the presence of chloride or bromide anions can in many cases interfere with the monitoring of electrochemical couples.

Visible–UV spectra were recorded on either a Varian 624 or Cary 210 spectrophotometer. IR spectra were obtained in KBr pellets or Nujol mulls on a Perkin-Elmer 224 grating infrared spectrometer. Magnetic susceptibilities of crystalline solids were measured at ambient temperature with a Faraday balance at Wright State University through the courtesy of Professor S. Cummings.

X-ray Characterization of *trans*-[Tc(DPPE)$_2$Br$_2$]BF$_4$. A red crystal of trigonal morphology with mean dimensions of 0.1 × 0.1 × 0.1 mm was mounted on a Syntex P2$_1$ diffractometer equipped with a graphite monochromator. Preliminary investigations using Cu Kα (1.541 78 Å) radiation indicated the diffraction symmetry to be trigonal. The lack of systematic absences suggested space groups $P3$ and $P\bar{3}$.[22] Space group $P\bar{3}$ was confirmed by subsequent solution and refinement of the structure. Crystal quality was checked by ω scans. Cell constants were determined by least-squares refinement using 20 values for 24 general high-angle reflections. These are a = 20.926 (5) Å and c = 11.178 (2) Å. With $Z = 3$, $d_{\text{calcd}} = 1.50$ g/cm^3 and $d_{\text{measd}} = 1.52$ g/cm^3. The rate for the θ–2θ scan varied between 6.0 and 24.0 °/min, depending on the intensity of the reflection being measured. Three reflections (400, 040, 003) were monitored to check for crystal stability and to account for long-term drift. These displayed only a random fluctuation with a maximum variation of 5%. The linear absorption coefficient (μ) was 35.08 cm^{-1}. Lorentz and polarization corrections were applied as well as an empirical absorption correction. A total of 3682 reflections were measured; of these, 3418 had intensities greater than 2σ, and only these were used in the solution and refinement of the structure.

Structure Solution and Refinement of *trans*-[Tc(DPPE)$_2$Br$_2$]BF$_4$. A Patterson vector map was computed, and the positions of the technetium and bromine atoms were determined. A Fourier map, which was calculated with the phases based on the Tc and Br positions, revealed all 28 independent non-hydrogen atoms of the cation. A subsequent difference Fourier map contained one ordered BF$_4^-$ on the 3-fold axis, and one disordered BF$_4^-$ ion on the $\bar{3}$ symmetry site. The disordered fluorine atoms were refined with fixed temperature factors (U = 0.15 Å^2). Anisotropic thermal parameters were used for all other non-hydrogen atoms, and hydrogen atoms were assigned isotropic thermal parameters corresponding to 1.2 times that of the atom to which each is bonded. In the final cycles of least-squares refinement 286 parameters were varied. Convergence was achieved with $R_1 = 0.0461$ and $R_2 = 0.0558$. In the last cycle of refinement the maximum shift per error was 0.08σ, and the average shift per error was 0.01σ. A difference Fourier map contained peaks corresponding to chemically reasonable positions for hydrogen atoms. Neutral-atom scattering curves were used for all atoms except hydrogen.[23] Corrections for anomalous dispersion were made for all non-hydrogen atoms.[23] The values of $|F_o|$ and F_c are listed in Table A.[24]

The program used in the solution of the structure was titled SHELXTL, a minicomputer package for crystal determination, by G. S. Sheldrick, Nicolet, XRD Division, 1981.

Results

Synthesis of the [TcD$_2$X$_2$]$^{+/0}$ Core. The TDP–technetium complexes can be prepared from TcO$_4^-$, TcOX$_4^-$, and TcX$_6^{2-}$ (X = Cl, Br) by reactions that involve net reduction of the technetium starting material. These reactions are illustrated below for the preparation of [Tc(DPPE)$_2$Cl$_2$]Cl. In each case the final product is identified by some combination of visible–UV, IR, or chromatographic (TLC, HPLC) techniques.

1. Reduction of TcO$_4^-$. When a solution of pertechnetate in either DMF/HCl or ethanol/HCl is heated with an excess of the TDP ligand DPPE, chromatographic purification of the reaction mixture leads to [Tc$^{\text{III}}$(DPPE)$_2$Cl$_2$]Cl. This reaction can be represented as

$$\mathrm{Tc^{VII}O_4^-} + \text{excess DPPE} \rightarrow \mathrm{Tc^{III}(DPPE)_2Cl_2^+} \qquad (1)$$

2. Reduction of Tc(O)Cl$_4^-$. When this starting material is stirred with an excess of DPPE in a solvent such as CH$_2$Cl$_2$ or ethanol and the resulting mixture is then allowed to stand at ambient temperature, small red crystals of [Tc(DPPE)$_2$Cl$_2$]Cl appear over a 2-day period.

$$\mathrm{Tc^{V}(O)Cl_4^-} + \text{excess DPPE} \rightarrow \mathrm{Tc^{III}(DPPE)_2Cl_2^+} \qquad (2)$$

3. Reduction of TcCl$_6^{2-}$. When a (hexahalogenato)technetate(IV) salt is dissolved in either DMF or ethanol and heated in the presence of at least 10-fold excess DPPE, the initial product formed is [Tc(DPPE)$_2$X$_2$]X, and the reaction can be represented as

$$\mathrm{Tc^{IV}Cl_6^{2-}} + \text{excess DPPE} \rightarrow \mathrm{Tc^{III}(DPPE)_2Cl_2^+} \qquad (3)$$

However, under the typical reaction conditions employed (high temperature and long reaction time) a further reduction to the neutral Tc(II) moiety often occurs. This can be represented as

$$\mathrm{Tc^{III}(DPPE)_2Cl_2^+} + \text{excess DPPE} \rightarrow \mathrm{Tc^{II}(DPPE)_2Cl_2^0} \qquad (4)$$

During this reduction the core of the molecule remains essentially undisturbed, and the gain or loss of an electron from this core is reversible (vide infra). In these reactions of TcX$_6^{2-}$, the transition from Tc(IV) to Tc(III) and then to TcII) occurs more rapidly when the starting material is TcBr$_6^{2-}$ than when it is TcCl$_6^{2-}$. However, the Tc(DPPE)$_2$Cl$_2^0$ neutral species has less of a tendency to air oxidize to the Tc(III) form than does the dibromo congener.

Davison and Jones[20] have recently reported that [Tc(DPPE)$_2$Cl$_2$]$^+$ can be prepared by direct substitution of DPPE onto the Tc(III) complex [Tc(tu)$_6$]Cl$_3$ in alcoholic HCl. We have confirmed this report and the following substitution reaction gives reasonable yields of [Tc(DPPE)$_2$Cl$_2$]Cl:

$$\mathrm{Tc^{III}(tu)_6^{3+}} + \text{excess DPPE} \rightarrow \mathrm{Tc^{III}(DPPE)_2Cl_2^+} \qquad (5)$$

Modification of the [TcD$_2$X$_2$]$^{+/0}$ Core. When azide or cyanide is stirred with ethanolic [Tc(DPPE)$_2$X$_2$]$^+$ (X = Cl, Br), the cation is reduced to the divalent state with no apparent substitution occurring under the conditions of the reaction. When thiocyanate is stirred with an ethanolic solution of [Tc(DPPE)$_2$X$_2$]$^+$ (X = Cl, Br), depending on the specific reaction conditions, one of three products can result: (a) the Tc(II) complex Tc(DPPE)$_2$X$_2^0$ resulting from the reduction of the Tc(III) without substitution by SCN$^-$, (b) the reddish thiocyanate salt of the starting Tc(III) complex, [Tc(DPPE)$_2$X$_2$]SCN, which is less soluble in ethanol than is the original halide salt, or (c) the bis(thiocyanato)technetium(II) complex Tc(DPPE)$_2$(SCN)$_2^0$, which deposits as shiny, cubic, amber crystals from a purple solution. This formulation as neutral Tc(DPPE)$_2$(SCN)$_2^0$ is based on elemental analysis (Table I) of the isolated material and the fact that both bromine and concentrated HNO$_3$ oxidize this purple complex to produce an intensely blue species that exhibits a visible absorption of greater intensity than that of the purple species. This oxidized bis(thiocyanato)–technetium complex is unstable and after several hours visible–UV spectra indicate the presence of both the oxidized (blue, $\lambda_{\max}$ = 584 nm) and reduced (purple, $\lambda_{\max}$ = 534 nm) species; addition of sodium borohydride totally regenerates the purple species. The IR spectrum of Tc(DPPE)$_2$(SCN)$_2^0$ is described in Table III.

Halogen Exchange. Fergusson[17] reports the synthesis of [Tc(DPPE)$_2$Br$_2$]Br by substitution of Br$^-$ onto [Tc(DPPE)$_2$Cl$_2$]$^+$. However, the visible–UV spectrum that is reported for the product of this substitution reaction ($\lambda_{\max}$ = 487 nm) does not agree with the visible–UV spectrum of the

---

[22] "International Tables for X-Ray Crystallography", 3rd ed.; Kynoch Press: Birmingham, England, 1974; Vol. IV.

[23] Iber, J. A.; Hamilton, W. C. "International Tables for X-Ray Crystallography"; Kynoch Press: Birmingham, England, 1974; Vol. IV.

[24] All tables designated by alphabetic characters have been deposited as supplementary material.

Table III. Infrared Spectrophotometric Parameters for Selected Technetium Complexes of Tertiary Diphosphines[a]

$Tc^{II}(DPPE)_2(SCN)_2{}^0$	3500 (br), 2060 (v, sh), 1445 (m), 1100 (br), 755 (m), 708 (s), 540 (m), 520 (sh)
$[Tc^{III}(DPPE)_2Cl_2]SCN$	3450 (br), 3060 (w), 2063 (v), 1590, 1580 (d), 1490 (m), 1440 (s), 1415 (sh), 1320 (w), 1200 (w), 1200 (2), 1165 (w), 1100 (s), 1035 (w), 1010 (w), 880 (w), 820 (w), 750 (s), 700 (s), 680 (sh), 660 (sh), 625 (sh), 540 (s), 520 (sh), 435 (w), 360 (d)
$[Tc^{III}(DPPE)_2Cl_2]Cl$	3400 (br), 1490 (s), 1425 (sh), 1415 (sh), 1320 (m), 1200 (m), 1095 (s), 1005 (m), 875 (m), 830 (m), 805 (s), 700 (s), 680 (sh), 660 (sh), 540 (s), 490 (m), 360 (m)

[a] Spectra obtained in Nujol mulls or KBr pellets. Band positions reported in cm^{-1}. br = broad, s = strong, m = medium, w = weak, v = very strong, sh = shoulder, and d = doublet.

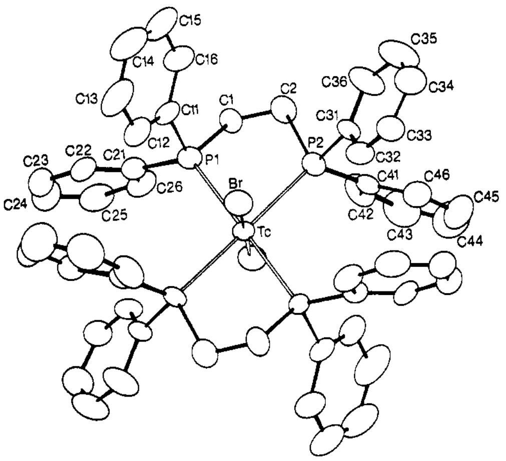

Figure 1. Perspective view of the *trans*-$[Tc(DPPE)_2Br_2]^+$ cation (50% ellipsoids shown; hydrogen atoms omitted for clarity).

compound synthesized in this work by the substitution of DPPE onto $TcBr_6{}^{2-}$ (λ_{max} = 504 nm). Single-crystal structural analysis of this latter material (vide infra) shows that it does indeed contain the $[Tc(DPPE)_2Br_2]^+$ cation and thus the 504-nm maximum is characteristic of this cation. In order to clarify the discrepancy between Fergusson's results and ours, the Fergusson synthesis was reproduced exactly as reported and the products were characterized by visible–UV spectrophotometry and elemental analysis (see Experimental Section). The results indicate that $[Tc(DPPE)_2Br_2]^+$ cannot be quantitatively generated from $[Tc(DPPE)_2Cl_2]^+$ under the indicated reaction conditions. The actual products appear to be (a) a small amount of the dibromo substitution product and (b) a mixture of complexes having a Cl/Br ratio of 7/2. It was qualitatively observed that refluxing a 10-fold excess of Br^- with $[Tc(DPPE)_2Cl_2]^+$ in ethanol for as long as 20 h will not cause the spectral maximum to shift further toward the red than 487 nm. Conversely, refluxing $[Tc(DPPE)_2Br_2]^+$ with excess LiCl in ethanol for several hours causes a shift in the peak from 504 to 480 nm, this peak being characteristic for $[Tc(DPPE)_2Cl_2]^+$ (Table I).

Crystal Structure. Final fractional atomic positional parameters and their estimated standard deviations are given in Table IV. The corresponding anisotropic thermal parameters may be found in Table B,[24] and the associated ellipsoids for the complex cation are shown in Figure 1. Bond lengths and selected bond angles are found in Table V, with the remaining found in Table C.[24] Calculated hydrogen atom positions are in Table D.[24]

Table IV. Atom Coordinates ($\times 10^4$) and Temperature Factors ($Å^2 \times 10^3$) for $[Tc(DPPE)_2Br_2]BF_4$

atom	*x*	*y*	*z*	*U*
Tc	5000	0	0	29 (1)[a]
Br	4054 (1)	−550 (1)	1546 (1)	51 (1)[a]
P(1)	5160 (1)	1253 (1)	244 (1)	42 (1)[a]
P(2)	6018 (1)	509 (1)	1527 (1)	42 (1)[a]
C(1)	6125 (3)	1838 (3)	704 (5)	57 (3)[a]
C(2)	6342 (3)	1512 (3)	1664 (5)	62 (2)[a]
C(11)	4608 (3)	1352 (3)	1391 (4)	52 (3)[a]
C(12)	3824 (3)	903 (3)	1316 (5)	63 (3)[a]
C(13)	3383 (4)	991 (4)	2170 (6)	92 (5)[a]
C(14)	3740 (4)	1505 (4)	3111 (6)	90 (5)[a]
C(15)	4477 (4)	1903 (3)	3192 (5)	79 (4)[a]
C(16)	4926 (4)	1855 (3)	2347 (5)	63 (3)[a]
C(21)	5093 (3)	1764 (2)	−1018 (4)	44 (2)[a]
C(22)	4459 (3)	1800 (3)	−1229 (5)	57 (3)[a]
C(23)	4400 (4)	2150 (4)	−2247 (5)	68 (4)[a]
C(24)	4964 (4)	2464 (3)	−3055 (5)	66 (3)[a]
C(25)	5586 (4)	2427 (3)	−2872 (5)	66 (3)[a]
C(26)	5666 (3)	2095 (3)	−1861 (5)	59 (3)[a]
C(31)	5871 (3)	218 (3)	3082 (4)	51 (3)[a]
C(32)	5369 (3)	−491 (3)	3417 (5)	62 (3)[a]
C(33)	5318 (4)	−718 (3)	4592 (5)	70 (3)[a]
C(34)	5757 (4)	−246 (4)	5451 (5)	75 (4)[a]
C(35)	6251 (4)	468 (4)	5140 (5)	98 (4)[a]
C(36)	6318 (4)	692 (4)	3972 (5)	81 (3)[a]
C(41)	6861 (3)	470 (3)	1182 (5)	50 (2)[a]
C(42)	7357 (3)	942 (4)	353 (6)	71 (3)[a]
C(43)	7967 (4)	898 (4)	100 (7)	87 (4)[a]
C(44)	8094 (4)	382 (5)	622 (7)	92 (4)[a]
C(45)	7612 (4)	−82 (4)	1462 (7)	86 (4)[a]
C(46)	6988 (3)	−43 (3)	1760 (6)	66 (3)[a]
F(1)	6667	3333	2719 (4)	80 (2)
F(2)	6561 (3)	2674 (2)	4344 (4)	121 (2)
B(1)	6667	3333	3938 (4)	61 (3)
B(2)	0	0	0	150
F(3)	211 (9)	638 (7)	484 (10)	150
F(4)	0	0	−1170 (14)	150

[a] Equivalent isotropic *U* defined as one-third of the trace of the orthogonalized U^{ii} tensor.

Table V

Selected Bond Lengths (Å) in the *trans*-$[Tc(DPPE)_2Br_2]^+$ Cation

Tc–Br	2.440 (1)	C(1)–C(2)	1.460 (9)
Tc–P(1)	2.488 (1)		
Tc–P(2)	2.513 (1)		
P(1)–C(1)	1.836 (5)	P(2)–C(2)	1.860 (6)
P(1)–C(11)	1.805 (7)	P(2)–C(31)	1.817 (5)
P(1)–C(21)	1.816 (6)	P(2)–C(41)	1.846 (2)

Selected Bond Angles (deg) in the *trans*-$[Tc(DPPE)_2Br_2]^+$ Cation

Br–Tc–P(1)	94.0 (1)	P(1)–Tc–P(2)	80.8 (1)
Br–Tc–P(2)	92.0 (1)		

This structure consists of discrete cationic complexes and $BF_4{}^-$ anions separated by typical van der Waals distances. One of the crystallographically distinct $BF_4{}^-$ anions is well-behaved, while the other is disordered. The B atom of this latter anion occupies the $\bar{3}$ symmetry site; in the disorder model the total electron density of the four F atoms is distributed over eight symmetry-related positions. The technetium(III) center is six-coordinate with an approximately octahedral coordination environment. The donor phosphorus atoms of the two bidentate TDP ligands occupy the four equatorial coordination sites, while two bromine atoms occupy the two trans-axial positions. The bidentate coordination of the DPPE ligands to the Tc(III) center results in two five-membered chelate rings.

Colors. In the $Tc^{IV}X_6{}^{2-}$ series the chloro complex is yellow, the bromo complex is deep red, and the iodo analogue is black. The Tc(III) $[TcD_2X_2]^+$ chloro compounds are orange, orange-red, or red; the bromo analogues are a deeper red to rose color, some appearing almost violet. The Tc(II) $TcD_2X_2{}^0$

Table VI. Chromatographic Parameters for Selected Technetium-Diphosphine Complexes and Diphosphine Ligands[a]

HPLC

compd	retention time, min
$[Tc^{III}(DPPE)_2Cl_2]Cl$	10.3
$[Tc^{III}(DEPE)_2Cl_2]SO_3CF_3$	7.3
$[Tc^{III}(DEPE)_2Br_2]Br$	11.0
$[Tc^{III}(DMPE)_2Br_2]ReO_4$	7.3
$[Tc^{III}(DMPE)_2Cl_2]SO_3CF_3$	6.0
$[Tc^{III}(DPPB)_2Cl_2]Cl$	13.3
$[Tc^{III}(DPPB)_2Cl_2]BF_4$	13.3

TLC

compd	developing solvent	plate	R_f
$[Tc^{III}(DPPB)_2Cl_2]Cl$	95% EtOH	C_{18}	0.73
$[Tc^{III}(DPPB)_2Cl_2]Cl$	abs ethanol	silica	0.71
$[Tc^{III}(DPPB)_2Cl_2]Cl$	abs ethanol	alumina	0.71
$[Tc^{III}(DPPB)_2Br_2]Br$	95% ethanol	C_{18}	0.72
$[Tc^{III}(DPPB)_2Br_2]Br$	abs ethanol	silica	0.77
$[Tc^{III}(DPPE)_2Cl_2]Cl$	95% ethanol	C_{18}	0.79
$[Tc^{III}(DPPE)_2Br_2]Br$	95% ethanol	C_{18}	0.79
$[Tc^{III}(DPPV)_2Cl_2]Cl$	95% ethanol	C_{18}	0.74
$[Tc^{III}(DEPE)_2Cl_2]Cl$	abs ethanol	silica	0.60
$[Tc^{III}(DEPE)_2Cl_2]Cl$	95% ethanol	C_{18}	0.75
DPPB	toluene	silica	0.77
DPPB	abs ethanol	silica	0.85
DPPB	abs ethanol	C_{18}	0.50
DPPE	abs ethanol	C_{18}	0.62
DPPE	95% ethanol	C_{18}	0.51
DPPV	95% ethanol	C_{18}	0.50

[a] Conditions given in Experimental Section.

complexes are invariably yellow, gold-yellow, or green-yellow. The $Tc(DPPE)_2(SCN)_2$ complex is a rose-amber color as a solid but appears purple when dissolved in CH_2Cl_2.

Solubilities. Overall, the phenyl-substituted TDP–technetium(III) complexes are soluble in polar organic solvents such as ethanol, acetone, DMF, or Me_2SO. The analogous Tc(II) complexes are more soluble in nonpolar solvents such as toluene, benzene, pyridine, or CH_2Cl_2. When D = DPPE, both the Tc(II) and the Tc(III) species are very soluble in methylene chloride, the ligand itself having great solubility in this solvent. In general, the solubility of the $[TcD_2X_2]^{0/+}$ complexes reflects the solubility pattern of the coordinating TDP ligand; e.g., DPPE, $Tc(DPPE)_2X_2^0$, and $[Tc(DPPE)_2X_2]X$ are all very soluble in CH_2Cl_2. The least soluble of all the complexes results when D = DPPB. Alkyl- and phenyl-substituted TDP–technetium(III) complexes are soluble in reasonably polar solvents; the methyl- and ethyl-substituted congeners are additionally soluble in aqueous and aqueous/alcohol media.

Characterization. In addition to the single-crystal X-ray structural determination of the title complex, the TDP–technetium complexes are characterized by (1) elemental analyses of representative compounds, the results of which are in agreement with proposed formulations (Table I), (2) visible–UV and IR spectrophotometry (Tables II and III), and (3) HPLC and TLC analyses, which establish the chemical purity of the complexes. In the TLC analyses, all complexes migrated as a single spot with R_f values (Table VI) ranging from 0.6 to 0.8 and with no detectable excess ligand. Table VI also lists the observed HPLC retention times of some of the TDP–technetium complexes. Comparison of peak areas indicates that by HPLC analysis all complexes are greater than 90% pure and most are greater than 95% pure.

All the $[TcD_2D_2]^{0/+}$ complexes are paramagnetic. The measured magnetic moments of $Tc(DPPE)_2Br_2^0$ (1.88 μ_B) and $[Tc(DPPE)_2Br_2]Br$ (2.47 μ_B) are in the same range as those reported by Fergusson.[17]

Visible–UV Spectra. Spectrophotometric data for the $[TcD_2X_2]^{0/+}$ complexes are presented in Table II. These highly colored species all exhibit characteristic, well-defined, intense bands in the visible region. An examination of the data in Tables VII–X reveals the following trends: (a) For compounds of identical ligand environments this band consistantly occurs at a higher energy for Tc(II) complexes than for Tc(III) complexes. The average difference for 11 pairs of complexes is 2500 ± 370 cm^{-1} (Table VII). (b) For compounds identical in all respects except in the nature of the trans halogen ligands, this band occurs at a higher energy for the dichloro complex than for the dibromo complex. The average difference for 8 pairs of complexes is 1550 ± 270 cm^{-1} (Table VIII). (c) Within a related series, this band occurs at higher energy for

Table VII. Variation in the Energy of the HTTCT (Halogen-to-Technetium-Charge-Transfer) Transition for $[TcD_2X_2]^{+/0}$ Complexes as a Function of Technetium Oxidation State

compd	λ_{max}, cm^{-1}	$\lambda_{max}^{III} - \lambda_{max}^{II}$, cm^{-1}
$Tc^{III}(DPPE)_2Cl_2^+$ $Tc^{II}(DPPE)_2Cl_2^0$	20 833 23 810	2977
$Tc^{III}(DPPE)_2Br_2^+$ $Tc^{II}(DPPE)_2Br_2^0$	19 841 22 026	2185
$Tc^{III}(DPPV)_2Cl_2^+$ $Tc^{II}(DPPV)_2Cl_2^0$	21 053 23 858	2532
$Tc^{III}(DPPB)_2Cl_2^+$ $Tc^{II}(DPPB)_2Cl_2^0$	20 325 22 831	2506
$Tc^{III}(DIARS)_2Cl_2^+$ $Tc^{II}(DIARS)_2Cl_2^0$	22 883 25 445	2562
$Tc^{III}(DIARS)_2Br_2^+$ $Tc^{II}(DIARS)_2Br_2^0$	21 186 23 753	2567
$Tc^{III}(DPPE)_2(SCN)_2^+$ $Tc^{II}(DPPE)_2(SCN)_2^0$	17 123 18 727	1604
$Tc^{III}(DEPE)_2Cl_2^+$ $Tc^{II}(DEPE)_2Cl_2^0$	21 413 24 390	2977
$Tc^{III}(DEPE)_2Br_2^+$ $Tc^{II}(DEPE)_2Br_2^0$	20 284 22 831	2547
$Tc^{III}(DMPE)_2Cl_2^+$ $Tc^{II}(DMPE)_2Cl_2^0$,	21 598 24 155	2557
$Tc^{III}(DMPE)_2Br_2^+$ $Tc^{II}(DMPE)_2Br_2^0$	20 121 22 779	2658

Table VIII. Variation in the Position of the HTTCT Transition for $[TcD_2X_2]^{+/0}$ Complexes as a Function of the trans Halogen Ligands

compd	λ_{max}, cm^{-1}	$\lambda_{max}^{Br} - \lambda_{max}^{Cl}$, cm^{-1}
$Tc^{II}(DPPE)_2Br_2^0$ $Tc^{II}(DPPE)_2Cl_2^0$	22 026 23 810	1784
$Tc^{II}(DPPV)_2Br_2^0$ $Tc^{II}(DPPV)_2Cl_2^0$	21 692 23 585	1893
$Tc^{II}(DPPB)_2Br_2^0$ $Tc^{II}(DPPB)_2Cl_2^0$	21 254 22 831	1577
$Tc^{II}(DEPE)_2Br_2^0$ $Tc^{II}(DEPE)_2Cl_2^0$	22 831 24 390	1559
$Tc^{II}(DMPE)_2Br_2^0$ $Tc^{II}(DMPE)_2Cl_2^0$	22 779 24 155	1376
$Tc^{II}(DIARS)_2Br_2^0$ $Tc^{II}(DIARS)_2Cl_2^0$	23 753 25 445	1692
$Tc^{III}(DIARS)_2Br_2^+$ $Tc^{III}(DIARS)_2Cl_2^+$	21 186 22 883	1697
$Tc^{III}(DPPE)_2Br_2^+$ $Tc^{III}(DPPE)_2Cl_2^+$	19 841 20 833	992
$Tc^{III}(DEPE)_2Br_2^+$ $Tc^{III}(DEPE)_2Cl_2^+$	20 283 21 552	1269
$Tc^{III}(DMPE)_2Br_2^+$ $Tc^{III}(DMPE)_2Cl_2^+$	20 121 21 739	1618

Table IX. Variation in the Position of the HTTCT Transition for $[\mathrm{TcD_2X_2}]^{+/0}$ Complexes as a Function of the Substituents on the Donor Phosphorus Atoms

compd	substituent	$\lambda_{\max}$, cm^{-1}
$\mathrm{Tc^{III}Cl_2(DPPE)_2{}^+}$	phenyl	20 833
$\mathrm{Tc^{III}Cl_2(DEPE)_2{}^+}$	ethyl	21 552
$\mathrm{Tc^{III}Cl_2(DMPE)_2{}^+}$	methyl	21 739
$\mathrm{Tc^{III}Br_2(DPPE)_2{}^+}$	phenyl	19 841
$\mathrm{Tc^{III}Br_2(DEPE)_2{}^+}$	ethyl	20 283
$\mathrm{Tc^{III}Br_2(DMPE)_2{}^+}$	methyl	20 121
$\mathrm{Tc^{II}Br_2(DPPE)_2{}^0}$	phenyl	22 026
$\mathrm{Tc^{II}Br_2(DEPE)_2{}^0}$	ethyl	22 831
$\mathrm{Tc^{II}Br_2(DMPE)_2{}^0}$	methyl	22 779
$\mathrm{Tc^{II}Cl_2(DPPE)_2{}^0}$	phenyl	23 810
$\mathrm{Tc^{II}Cl_2(DEPE)_2{}^0}$	ethyl	24 390
$\mathrm{Tc^{II}Cl_2(DMPE)_2{}^0}$	methyl	24 155

Table X. Variation in the Position of the HTTCT Transition for $[\mathrm{TcD_2X_2}]^{+/0}$ Complexes as a Function of the Backbone of the Bidentate Diphosphine Ligand

compd	backbone	$\lambda_{\max}$, cm^{-1}
$\mathrm{Tc^{II}Cl_2(DPPE)_2{}^0}$	ethane	23 810
$\mathrm{Tc^{II}Cl_2(DPPV)_2{}^0}$	ethylene	23 585
$\mathrm{Tc^{II}Cl_2(DPPB)_2{}^0}$	*o*-phenylene	22 831
$\mathrm{Tc^{II}Br_2(DPPE)_2{}^0}$	ethane	22 026
$\mathrm{Tc^{II}Br_2(DPPV)_2{}^0}$	ethylene	21 692
$\mathrm{Tc^{II}Br_2(DPPB)_2{}^0}$	*o*-phenylene	21 254
$\mathrm{Tc^{III}Cl_2(DPPE)_2{}^+}$	ethane	20 833
$\mathrm{Tc^{III}Cl_2(DPPV)_2{}^+}$	ethylene	21 053
$\mathrm{Tc^{III}Cl_2(DPPB)_2{}^+}$	*o*-phenylene	20 325

the alkyl-substituted TDP complexes than for the corresponding phenyl-substituted TDP complexes, the difference being ca. 600 cm^{-1} (Table IX). (d) For the series $\mathrm{TcD_2X_2}^0$, when the trans halogen is held constant for a given series, the energy of this band decreases in the order DPPE, DPPV, DPPB (Table X) (range of 1000 cm^{-1} for X = Cl and ca. 800 cm^{-1} for X = Br). (e) For the comparable Tc(III) series $[\mathrm{TcD_2Cl_2}]^+$ the energy of this band decreases in the order DPPV, DPPE, DPPB (Table X) (range ca. 700 cm^{-1}). Tables VII–X summarize the relevant data as a function of (a) the metal oxidation state, (b) the nature of the axial substituent, (c) the composition of the carbon backbone uniting the equatorial donor atoms, and (d) the substituents on the donor phosphorus atoms.

Cyclic Voltammetry. All of the TDP–technetium complexes investigated herein are characterized by a Tc(III)/Tc(II) redox couple (Table XI). This redox couple is assigned as reversible on the basis of the following criteria: (1) The separation between the cathodic and anodic peaks in the voltammogram is close to the Nernstian value of 59 mV. The observed peak separations range from 57 to 82 mV, with the average being 67 mV (a typical cyclic voltammogram is shown in Figure 2). (2) The ratio of anodic peak current to cathodic peak current is nearly unity. (3) The peak current is proportional to the square root of the scan rate. $E^{\circ\prime}$ was calculated by averaging E_{pc} (potential of maximum cathodic current) and E_{pa} (potential of maximum anodic current).

The data in Table XI reveal the following trends: (a) When complexes having identical equatorial ligands are compared, the $E^{\circ\prime}$ of the $[\mathrm{TcD_2Br_2}]^{0/+}$ couple is about 100 mV more positive than the $E^{\circ\prime}$ of the corresponding dichloro complex. (b) With respect to the equatorial ligand, the $E^{\circ\prime}$ values of the phenyl-substituted TDP–technetium complexes are about 250 mV more positive than those of the alkyl-substituted analogues. When both effects are combined, the range of observed Tc(III)/Tc(II) $E^{\circ\prime}$ values is from +392 to −250 mV (vs. Ag/AgCl).

Table XI. Reduction Potentials for Some Tc(III)/Tc(II) and Tc(II)/Tc(I) Couples in *N,N*-Dimethylformamide[a]

compd	$E^{\circ\prime}_{\mathrm{III/II}}$,[b] mV	$E^{\circ\prime}_{\mathrm{II/I}}$,[b] mV	E_{pc}[c]
$\mathrm{Tc(DPPE)_2(SCN)_2{}^{+/0/-}}$	+390	−600	
$\mathrm{Tc(DPPB)_2Cl_2{}^{+/0/-}}$	+92		−1080
$\mathrm{Tc(DPPE)_2Br_2{}^{+/0/-}}$	+103[d]		
$\mathrm{Tc(DPPE)_2Cl_2{}^{+/0/-}}$	−1		−1070
$\mathrm{Tc(DMPE)_2Br_2{}^{+/0/-}}$	−99	−1260	
$\mathrm{Tc(DMPE)_2Cl_2{}^{+/0/-}}$	−232	−1395	
$\mathrm{Tc(DEPE)_2Br_2{}^{+/0/-}}$	−138		−1420
$\mathrm{Tc(DEPE)_2Cl_2{}^{+/0/-}}$	−252		−1440

[a] Given in millivolts vs. Ag/AgCl. The supporting electrolyte is 0.5 M TEAP unless otherwise noted. [b] Reversible couple. [c] Peak potential for the irreversible cathodic wave. [d] Reference 29. Listed value (vs. Ag/AgCl) obtained by adding 35 mV to the reported value of 68 mV vs. NaSCE.

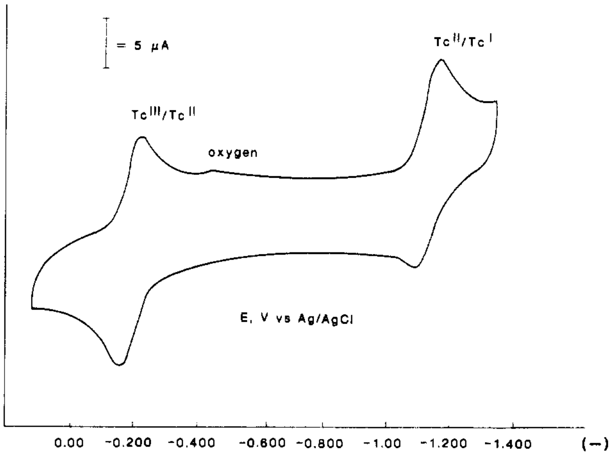

Figure 2. Cyclic voltammogram of 1.1 mM $[\mathrm{Tc(DMPE)_2Cl_2}]^+$. Conditions: 0.5 M TEAP in DMF; scan rate 50 mV/s; potential measured vs. Ag/AgCl.

Three of the TDP–technetium complexes, $[\mathrm{Tc(DPPE)_2(SCN)_2}]^{0/-}$, $[\mathrm{Tc(DMPE)_2Cl_2}]^{0/-}$, and $[\mathrm{Tc(DMPE)_2Br_2}]^{0/-}$, also exhibit a reversible Tc(II)/Tc(I) redox couple, the $E^{\circ\prime}$ values of which are ca. 1000 mV more negative than those of the corresponding Tc(III)/Tc(II) $E^{\circ\prime}$ values (Table XI). The remainder of the complexes investigated exhibit an irreversible, or a pseudoreversible, reduction of Tc(II) to Tc(I). The cathodic peak potential of this Tc(II)/Tc(I) process ranges from −0.97 to −1.45 V (vs. Ag/AgCl).

Under the conditions employed in this work, no oxidation from Tc(III) to Tc(IV) is observed for any of the $[\mathrm{TcD_2X_2}]^+$ complexes studied.

Discussion

Synthesis and Characterization. The technetium(III) $[\mathrm{TcD_2X_2}]^+$ complexes can be prepared by a variety of synthetic procedures, of which substitution onto a technetium(III) metal center (eq 5) is classic. Advantages of this type of nonredox synthesis include both minimization of the number of resulting products and also greater control over the nature (e.g., oxidation state, coordination number, and geometry) of those products. In the case where the technetium starting material is in a higher oxidation state than the Tc(III) product (eq 1–3), the reactions are conducted in excess D and the ligand both reduces and coordinates to the technetium center. The fact that the $[\mathrm{TcD_2X_2}]^+$ products can be generated directly from pertechnetate is important from the point of view of nuclear medicine. Essentially all reduced $^{99\mathrm{m}}$Tc radiopharmaceuticals are derived in one fashion or another from the $^{99\mathrm{m}}\mathrm{TcO_4}^-$ eluted from a ^{99}Mo/$^{99\mathrm{m}}$Tc generator.[7] It is interesting to note that the same complex, e.g. $[\mathrm{Tc(DPPE)_2X_2}]^{+/0}$, can be prepared from four different starting materials in four different oxiation states. This is a relatively rare situation in technetium chemistry, indicating that in this system the desired product complex is also the thermodynamically stable product.

Purification of the $TcD_2X_2^+$ complexes largely involves removing the Tc(II) analogue, $TcD_2X_2^0$, produced by the presence of excess reductant (i.e., excess D) in the reaction mixture (eq 4). However, the chemical differences between the Tc(III) salt and the neutral Tc(II) compound can also be exploited in synthetic procedures by generating the desired moiety in a medium in which it has little or no solubility. For example, a solution of $TcD_iX_2^0$, which has been dissolved in some reasonably nonpolar solvent, can be oxidized to yield an insoluble salt of $[TcD_2X_2]^+$; or an ethanolic solution of $[TcD_2X_2]^+$ can be reduced to yield the insoluble $TcD_2X_2^0$.

Synthetic modification of the $[TcD_2X_2]^+$ core via displacement of the trans-axial halogens is complicated by the fact that the Tc(III) metal center is amenable to further reduction and that the pseudohalogen nucleophiles employed in this study are reasonably good reductants. The three pseudohalides, azide, cyanide, and thiocyanate, all reduce the Tc center of $[Tc(DPPE)_2X_2]^+$ from III to II. Thiocyanate is further able to displace the axial halides, resulting in the formation of $Tc(DPPE)_2(SCN)_2^0$, which is characterized by elemental analysis (Table I). Although infrared spectroscopy has often been useful in determining the bonding mode of coordinated thiocyanate,[25] comparison with the infrared spectrum of the thiocyanate salt $[Tc(DPPE)_2Cl_2](SCN)$ (Table III) shows that the ν_{CN} stretching frequency at 2080 cm^{-1} is similar in both materials. Thus, the bonding mode of thiocyanate in $Tc(DPPE)_2(SCN)_2^0$ cannot be assigned from these IR data.

Extremely stringent reaction conditions are required to cause displacement of the halide ligands of the *trans*-$[Tc^{III}D_2X_2]^+$ complexes. For example, refluxing $[Tc(DPPE)_2Cl_2]^+$ with 0.026 M LiBr in 83% ethanol for 6 h leads to only ca. 15% exchange of bromide for chloride. Thus, the $[Tc^{III}D_iX_2]^+$ complexes can definitely be characterized as substantially robust, expecially in those cases where D is a phenyl-substituterd TDP ligand.

The robust character of the $[TcD_2X_2]^+$ center makes it difficult to prepare these complexes by halogen-exchange reactions. In our hands $[Tc(DPPE)_2Cl_2]^+$ cannot be converted to $[Tc(DPPE)_2Br_2]^+$ by refluxing with LiBr in ethanol, conditions reported to be successful by Fergusson.[17] However, $[Tc(DPPE)_2Br_2]^+$ can be converted to $[Tc(DPPE)_2Cl_2]^+$ by refluxing with LiCl in ethanol. These apparently disparate results are rationalized on the basis that in this system, as in many others,[26] the M–Br bond is more labile than is the M–Cl bond, and/or the dichloro complex is thermodynamically more stable than is the dibromo complex. To avoid the possibility of generating mixed-halogen products, halogen-exchange reactions were not used synthetically in this work. Instead, the $[TcD_2X_2]^+$ complexes were generated from the analogous TcX_6^{2-} starting materials or from the equivalent TcO_4^- plus HX combinations.

Crystal Structure. The overall structure of the $[Tc(DPPE)_2Br_2]^+$ cation is as expected on the basis of the recently reported structural analysis of the related diarsine complex $[Tc(DIARS)_2Cl_2]^{+}$[27] and on the basis of a brief description of the structure of the analogous complex $[Tc(DMPE)_2Cl_2]^+$.[13] All three of these Tc(III) species exhibit trans-substituted, approximately octahedral geometries. This geometry is universally observed for $[M(DIARS)_2X_2]^{n+}$ complexes[28] and is expected to be very common for $[MD_2X_2]^{n+}$ complexes, where D is either a tertiary chelating diphosphine or diarsine ligand. Presumably, in these complexes steric interactions among the bulky D ligands cause the trans configuration to be significantly favored over the cis configuration.

The average Tc(III)–P bond distance in $[Tc(DPPE)_2Br_2]^+$ is 2.50 (2) Å whereas the Tc(III)–P bond distance reported for $[Tc(DMPE)_2Cl_2]^+$ is significantly shorter at 2.436 Å. Determination of whether this difference results from the greater steric requirements of the phenyl groups of the DPPE ligand (relative to the methyl groups of the DMPE ligand) or from greater π-back-bonding from Tc(III) to P in the $[Tc(DPPE)_2Br_2]^+$ complex will have to await further detailed structural analyses of related complexes.

Visible–UV Spectra. The characteristic charge-transfer absorption associated with each of the $[TcD_2X_2]^{+/0}$ complexes investigated is assigned as arising from a halogen-to-technetium charge-transfer transition (HTTCT) since the energy at which this absorption occurs is primarily dependent on the technetium oxidation state and on the nature of the trans-axial halogens. These dependences can be understood within the tenets underlying charge-transfer phenomena. Thus, for analogous Tc(III) and Tc(II) complexes the HTTCT occurs at lower energy for Tc(III) since Tc(III) is a better oxidant than Tc(II). Also, for analogous bromo and chloro complexes the HTTCT occurs at lower energy for Br since bromide is a better reductant than is chloride. Consistent with this assignment, the energy of the HTTCT band is only slightly affected by alterations in the equatorial coordination environment provided by the four donor phosphorus atoms. These relatively minor effects induced by varying the nature of D are consistent with the prevailing view of π-back-bonding in phosphine complexes of low-valent metals. Within this view, metal–phosphorus bonding involves both σ-bonding of sp^3-hybridized P atom orbitals to the metal and π-back-bonding from metal t_{2g} orbitals to appropriately located, empty 3d P orbitals. When the tertiary phosphine is a good σ donor (i.e., when the substituents on the phosphorus atom are alkyl groups), the HTTCT is more difficult to effect (higher energy) since increased electron density on the technetium center makes it a poorer oxidant. As the substituents and carbon backbone of the TDP ligand are modified to render it more π-acidic, and thus remove electron density from the technetium center, the HTTCT becomes more accessible (lower energy). These trends may be summarized as follows: with respect to the ability of the phosphine ligand substituents to inhibit HTTCT, the order is alkyl > phenyl; with respect to the carbon bridge joining the P atoms, the order is ethane $\simeq$ ethylene > *o*-phenylene.

Of all the $[TcD_2X_2]^{+/0}$ complexes investigated, the thiocyanato derivatives $[Tc(DPPE)_2(SCN)_2]^{+/0}$ exhibit charge-transfer transitions with the lowest observed energies, the maxima for the Tc(II) and Tc(III) complexes occurring at 534 and 584 nm, respectively. This low energy is qualitatively consistent with the above noted dependency of the HTTCT energy on the nature of X. However, the large magnitude of the change in transition energy which occurs on varying X from bromide to thiocyanate (i.e., 3370 cm^{-1} for the Tc(II) complex and 2720 cm^{-1} for the Tc(III) complex) indicates that other factors are involved in determining the energy of transitions exhibited by the $[Tc(DPPE)_2(SCN)_2]^{+/0}$ complexes.

Cyclic Voltammetry. The data of Table XI show that the excursion in $E^{\circ\prime}$ values for all $[TcD_2X_2]^{+/0}$ couples is 642 mV;

---

(25) Burmeister, J. L. "The Chemistry and Biochemistry of Thiocyanic Acid and its Derivatives"; Newmon, A. A., Ed.; Academic Press: London, 1975.

(26) Wilkins, R. G. "The Study of Kinetics and Mechanism of Reactions of Transition Metal Complexes"; Allyn and Bacon: Boston, MA, 1974.

(27) Elder, R. C.; Whittle, R.; Glavan, K. A.; Johnson, J. F.; Deutsch, E. *Acta Crystallogr. Sect. B B36* **1980**, 1662–1665.

(28) Alyea, E. C. "Transition Metal Complexes of Phosphorus, Arsenic and Antimony Ligands"; McAuliffe, C. A., Ed.; Wiley: New York, 1973; pp 309–373.

even when only the chloro and bromo complexes are considered, the excursion is 455 mV. Thus, the ligand environment of the complex exerts a dramatic influence on the ease with which electrons are transferred at the metal center. The extent of this influence can be appreciated by comparison of the 642-mV $E^{\circ\prime}$ excursion of Table XI to the difference in $E^{\circ\prime}$ between analogous Tc and Re complexes. For a variety of such complexes, in a variety of oxidation states, the difference in $E^{\circ\prime}$ between Tc and Re is only in the range 250–350 mV.[29] Thus, varying the ligand environment of $[MD_2X_2]^+$ complexes engenders a considerably larger change in the M(III)/M(II) $E^{\circ\prime}$ value than does even varying the identity of M from Tc to Re.

For $[TcD_2X_2]^+$ complexes, the Tc(III)/Tc(II) $E^{\circ\prime}$ value is a function of both the nature of the trans-axial halogen and of the nature of the substituents on the donor phosphorus atoms. For complexes with identical D ligands, the bromo species are stronger oxidants than the chloro analogues. For complexes with identical halogen ligands, those species containing aryl substituents on the donor P atoms are stronger oxidants than the analogues with alkyl substituents. The fact that $[TcD_2X_2]^+$ complexes are easier to reduce when X is Br (rather than Cl) has been noted previously[30] for D = DPPE and D = DIARS and is understood in terms of bromide being a better π-back-bonding ligand than chloride; the bromo ligand presumably stabilizes spin-paired d^5 Tc(II) relative to spin-paired d^4 Tc(III) by increased acceptance of t_{2g} electron density. The same effect appears in the Tc(II)/Tc(I) redox couples observed in the $[Tc(DMPE)_2X_2]^{0/-}$ (X = Cl, Br) system, the magnitude of the effect being equivalent to that observed in the Tc(III)/Tc(II) comparisons, i.e. ca. 100 mV. Variation of the substituents on the P atoms of the TDP ligands (alkyl vs. aryl) results in even larger differences in Tc(III)/Tc(II) values, i.e. ca. 250 mV. Again, this is understood in terms of π-back-bonding; considering the strong *p*-acid character of the phosphine ligand, it is not unreasonable that variations in this ligand should have greater effects on $E^{\circ\prime}$ than do variations in the weakly π-acidic trans-axial halogen ligands. The D ligands containing aryl substituents are better able to delocalize electron density and are thus stronger π-acids than those containing alkyl substituents. These ligands thus stabilize Tc(II) and cause the aryl-substituted $[TcD_2X_2]^+$ complexes to be stronger oxidants than the alkyl-substituted analogues.

The data in Table II show why under common laboratory conditions the thiocyanate complex $Tc(DPPE)_2(SCN)_2{}^0$ is stable in the Tc(II) state whereas the analogous chloro and bromo complexes are stable in the Tc(III) state. As expected, relative to bromide or chloride, thiocyanate stabilizes the lower oxidation states of technetium. Thus, reduction from Tc(III) to Tc(II) for $[Tc(DPPE)_2X_2]^+$ occurs ca. 400 mV more easily when X = SCN than when X = Cl and ca. 300 mV more easily when X = SCN than when X = Br. The same effect can be seen in the Tc(II)/Tc(I) couples, although the limited number of reversible Tc(II)/Tc(I) couples available makes the comparison less direct. From data for Tc(III)/Tc(II) couples, it is seen that DPPE complexes are more easily reduced than DMPE complexes by ca. 230 mV. On the assumption that this factor roughly carries over to Tc(II)/Tc(I) couples, it can be estimated from the data in Table II that reduction from Tc(II) to Tc(I) occurs ca. 565 mV more easily when X = SCN than when X = Cl and ca. 430 mV more easily when X = SCN than when X = Br.

Relationship between $E^{\circ\prime}$ and HTTCT Energy. For a given metal complex, both the potential at which the central metal undergoes reduction and the energy of any ligand-to-metal charge-transfer transitions (E_{LTMCT}) are dependent on the oxidizing power of the metal center. Thus, if the contribution of the ligand (E_L) to E_{LTMCT} can be taken into account, for a series of related complexes there should be a linear relationship between redox potential and ($E_{LTMCT} - E_L$). Such a relationship has indeed been observed for tris(bipyridyl) complexes of several metals.[30,31] However, in most cases the contribution of the ligand to E_{LTMCT} cannot be directly taken into account. But even in these cases, if the ligand contribution remains relatively constant along a series of complexes, then a linear relationship between $E^{\circ\prime}$ and E_{LTMCT} can be expected. Just such relationships have been reported for the two series of complexes $[(NH_3)_5RuL]^{2+/3+}$, where L is either a pyridine or benzonitrile derivative.[32]

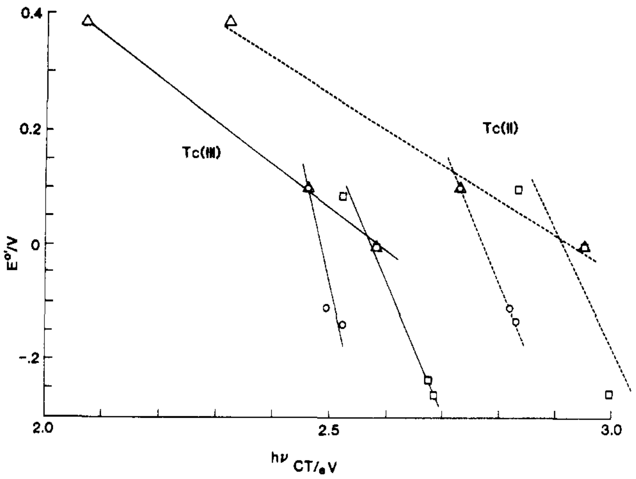

Figure 3. Plot of $E^{\circ\prime}$ for the reversible Tc(III)/Tc(II) couple in volts vs. the energy of the HTTCT (halogen-to-technetium-charge-transfer) transition in eV. Solid lines represent HTTCT energies for Tc(III) complexes while dashed lines represent HTTCT energies for Tc(II) complexes. Triangles represent variation of X ligands in $[Tc(DPPE)_2X_2]^{+/0}$ complexes. Circles represent variation of D ligands in $[TcD_2Br_2]^{+/0}$ complexes. Squares represent variation of D ligands in $[TcD_2Cl_2]^{+/0}$ complexes.

Figure 3 compares plots of the Tc(III)/Tc(II) $E^{\circ\prime}$ values vs. the energy of the halogen-to-technetium charge-transfer transition (E_{HTTCT}) for six series of related $[TcD_2X_2]^{+/0}$ complexes: for each of Tc(III) and Tc(II) there are plots wherein (a) X = Cl and D is varied, (b) X = Br and D is varied, and (c) D = DPPE and X is varied. Each plot is approximately linear; the four plots involving variations in D are approximately parallel to each other, while the two plots involving variations in X are approximately parallel to each other but not to the other four plots. The parallelism of related plots indicates that the effect of varying of a given ligand is roughly independent of the nature of the other ligands in the coordination sphere and independent of the technetium oxidation state. The fact that the two parallel plots describing variations in X have significantly lower slopes (ca. 0.7) than do the four plots describing variations in D (slopes ca. 2.5) indicates that E_{HTTCT} is more sensitive to variations in X while $E^{\circ\prime}$ is more sensitive to variations in D. This is exactly as expected from the character of the HTTCT transition, which is strongly dependent on the nature of X, and from the previously presented π-back-bonding arguments, indicating that $E^{\circ\prime}$ is strongly dependent on the nature of the D ligand.

---

(29) Hurst, R. W.; Heineman, W. R.; Deutsch, E. *Inorg. Chem.* **1981**, *20*, 3298.

(30) Saji, T.; Aoyagi, J. *J. Electroanal. Chem.* **1975**, *60*, 1.

(31) Matsumura-Inoue, T.; Tomono, H.; Kasai, M.; Tominaga-Morimoto, T. *J. Electroanal. Chem.* **1979**, *95*, 109.

(32) Matsubara, T.; Ford, P. C. *Inorg. Chem.* **1976**, *15*, 1107.

Inorg. Chem. **1983**, *22*, 1704–1707

Acknowledgment. Financial support by the National Institutes of Health (Grant No. HL-21276) and the Squibb Institute for Medical Research is gratefully acknowledged. We also thank Professor W. R. Heineman and Dr. A. Ichimura for helpful discussions concerning the electrochemical measurements.

Registry No. Tc(DPPE)$_2$(SCN)$_2$, 85552-63-2; Tc(DPPE)$_2$Cl$_2$, 78656-00-5; Tc(DPPE)$_2$Br$_2$, 85552-64-3; Tc(DPPB)$_2$Cl$_2$, 85552-65-4; Tc(DPPV)$_2$Br$_2$, 85552-66-5; Tc(DPPV)$_2$Cl$_2$, 85552-67-6; Tc(DEPE)$_2$Cl$_2$, 85552-68-7; Tc(DMPE)$_2$Cl$_2$, 85552-69-8; Tc(DEPE)$_2$Br$_2$, 85552-70-1; Tc(DMPE)$_2$Br$_2$, 85552-71-2; [Tc(DPPV)$_2$Cl$_2$]BF$_4$, 85552-73-4; [Tc(DPPE)Cl$_2$]Cl, 85552-74-5; [Tc(DPPB)$_2$Cl$_2$]Cl, 85552-75-6; [Tc(DPPV)$_2$Cl$_2$]Cl, 85552-76-7; [Tc(DMPE)$_2$Cl$_2$]SO$_3$CF$_3$, 85552-78-9; [Tc(DMPE)$_2$Br$_2$]SO$_3$CF$_3$, 85552-80-3; [Tc(DPPE)$_2$Cl$_2$]SCN, 85552-81-4; [Tc(DPPE)$_2$Br$_2$]BF$_4$, 85552-82-5; [Tc(DEPE)$_2$Cl$_2$]SO$_3$CF$_3$, 85552-84-7; [Tc(DEPE)$_2$Br$_2$]Br, 85552-85-8; [Tc(DMPE)$_2$Br$_2$]ReO$_4$, 85552-86-9; [Tc(DPPE)$_2$Br$_2$]Br, 85552-87-0; Tc(DMPE)$_2$Cl$_2^-$, 85565-21-5; [Tc(DPPB)$_2$Cl$_2$]BF$_4$, 85552-89-2; [Tc(DPPB)$_2$Br$_2$]Br, 85552-90-5; [Tc(DEPE)$_2$Cl$_2$]Cl, 85552-91-6; Tc(DIARS)$_2$Cl$_2$, 14127-29-8; Tc(DIARS)$_2$Cl$_2^+$, 47512-11-8; Tc(DIARS)$_2$Br$_2^+$, 78610-19-2; Tc(DIARS)$_2$Br$_2$, 78610-21-6; Tc(DPPE)$_2$Br$_2$, 78656-01-6; Tc(DPPE)$_2$(SCN)$_2^+$, 85552-92-7; Tc(DPPE)$_2$(SCN)$_2^-$, 85552-93-8; Tc(DMPE)$_2$Br$_2^-$, 85552-94-9; [Tc(DPPE)$_2$Br$_2$]NO$_3$, 85552-95-0.

Supplementary Material Available: Tables A–D, showing F_c and F_o values, anisotropic thermal parameters, complete bond lengths and angles, and calculated hydrogen atom positions (25 pages). Ordering information is given on any current masthead page.

Contribution from the Department of Chemistry and Molecular Structure Center,
Indiana University, Bloomington, Indiana 47405

Reactions of Mo$_2$(OR)$_6$ (M≡M) Compounds (R = *i*-Pr and *t*-Bu) with Benzoyl Peroxide

MALCOLM H. CHISHOLM,* JOHN C. HUFFMAN, and CHARLES C. KIRKPATRICK

Received October 19, 1982

Hydrocarbon solutions of Mo$_2$(OR)$_6$ (M≡M) compounds, where R = *i*-Pr and *t*-Bu, react with benzoyl peroxide to give intensely blue solutions. Where R = *i*-Pr, a blue crystalline product has been isolated and is formulated as Mo$_2$(O-*i*-Pr)$_6$(O$_2$CPh)$_2$ (M=M) on the basis of analytical and spectroscopic data. A structure involving two edge-sharing octahedral units is proposed for the central Mo$_2$O$_{10}$ moiety: a pair of O-*i*-Pr ligands provide the bridging groups. Where R = *t*-Bu, the initially formed blue solution gives rise to a pale yellow-green crystalline product Mo$_2$(O-*t*-Bu)$_4$(O$_2$CPh)$_2$ (M≡M) and an uncharacterized purple paramagnetic molybdenum-containing compound. These products are proposed to arise from decomposition (disproportionation) of Mo$_2$(O-*t*-Bu)$_6$(O$_2$CPh)$_2$ (M=M). The Mo$_2$(O-*t*-Bu)$_4$(O$_2$CPh)$_2$ compound has been characterized by a single-crystal study and is shown to be closely related to the previously characterized compound Mo$_2$(O-*t*-Bu)$_4$(O$_2$CO-*t*-Bu)$_2$. The Mo≡Mo bond, of distance 2.236 (2) Å, is spanned by a pair of cis-bridging O$_2$CPh groups, Mo–O = 2.14 (2) Å (averaged). The two *t*-BuO ligands attached to each molybdenum atom, Mo–O = 1.88 (2) Å (averaged), complete the roughly square-planar coordination geometry for each MoO$_4$ unit. The overall Mo$_2$O$_8$ geometry is slightly skewed to avoid an eclipsing of the bulky *t*-BuO ligands. Crystal data for Mo$_2$(O-*t*-Bu)$_4$(O$_2$CPh)$_2$: space group *C*2/*c*, a = 21.43 (1) Å, b = 14.006 (6) Å, c = 12.299 (5) Å, β = 113.75 (1)°, Z = 4, and d_{calcd} = 1.428 g cm^{-3}.

Introduction

The M–M triple bond of configuration $\sigma^2\pi^4$ in compounds of formula M$_2$(OR)$_6$, where M = Mo or W and R = a bulky alkyl group such as *t*-Bu, *i*-Pr, or CH$_2$-*t*-Bu, is a reactive inorganic functionality. Stepwise transformations of bond order, 3 → 4, 3 → 2 → 1, and even cleavage, 3 → 0, have been observed. Simple adducts involving C≡O,[2] RC≡CR,[3] Me$_2$NC≡N,[4] and R$_2$CN$_2$[5] have been isolated, and trinuclear[6] and tetranuclear clusters[7] have been obtained from condensation or oligomerization reactions. In the dinuclear chemistry of molybdenum and tungsten, the M–M double bond is relatively rare, at least when compared to quadruple, triple, and single bonds.[8] In part this may reflect a lability of the $\sigma^2\pi^2$ configuration toward oxidation, although one cannot be dogmatic on this point since detailed studies are lacking. However, in the simple oxidative-addition reaction sequence depicted by eq 1, only where X = O-*i*-Pr was it possible to isolate the

$$\mathrm{Mo_2(O\text{-}\mathit{i}\text{-}Pr)_6\ (M{\equiv}M) \xrightarrow{+X_2} Mo_2X_2(O\text{-}\mathit{i}\text{-}Pr)_6\ (M{=}M) \xrightarrow{+X_2} Mo_2X_4(O\text{-}\mathit{i}\text{-}Pr)_6} \tag{1}$$

Mo=Mo-containing compound of formula Mo$_2$X$_2$(O-*i*-Pr)$_6$. When X = Cl, Br, or I, reactions proceeded to give Mo$_2$X$_4$(O-*i*-Pr)$_6$ (M—M) compounds.[9]

Even the careful addition of 1 equiv of X$_2$ (X = Br or I), which gave initially blue or green solutions indicative of the Mo=Mo)$^{8+}$ unit, yielded ultimately orange solutions of a 1:1 mixture of Mo$_2$(O-*i*-Pr)$_6$ and Mo$_2$X$_4$(O-*i*-Pr)$_6$ compounds. This suggested that Mo$_2$X$_2$(O-*i*-Pr)$_6$ (M=M) compounds might be unstable with respect to disproportionation to Mo$_2$(O-*i*-Pr)$_6$ (M≡M) and Mo$_2$X$_4$(O-*i*-Pr)$_6$ (M—M) compounds. Reasoning that the Mo–Mo double bond might be

---

(1) Chisholm, M. H.; Rothwell, I. P. *Prog. Inorg. Chem.* **1982**, *29*, 1 and references therein.

(2) Chisholm, M. H.; Cotton, F. A.; Extine, M. W.; Kelly, R. L. *J. Am. Chem. Soc.* **1979**, *101*, 7645. Chisholm, M. H.; Huffman, J. C.; Leonelli, J.; Rothwell, I. P. *Ibid.* **1982**, *104*, 7030.

(3) Chisholm, M. H.; Folting, K.; Huffman, J. C.; Rothwell, I. P. *J. Am. Chem. Soc.* **1982**, *104*, 4389.

(4) Chisholm, M. H.; Kelly, R. L. *Inorg. Chem.* **1979**, *18*, 2321.

(5) Chisholm, M. H.; Folting, K.; Huffman, J. C.; Ratermann, A. L. *J. Chem. Soc., Chem. Commun.* **1981**, 1229.

(6) Chisholm, M. H.; Folting, K.; Huffman, J. C.; Kirkpatrick, C. C. *J. Am. Chem. Soc.* **1981**, *103*, 5967.

(7) Chisholm, M. H.; Errington, R. J.; Folting, K.; Huffman, J. C. *J. Am. Chem. Soc.* **1982**, *104*, 2025.

(8) Cotton, F. A.; Walton, R. A. "Multiple Bonds Between Metal Atoms"; Wiley: New York, 1982. Compounds containing $\mathrm{W\overset{4}{-}W}$ bonds are still quite rare.

(9) Chisholm, M. H.; Kirkpatrick, C. C.; Huffman, J. C. *Inorg. Chem.* **1981**, *20*, 871.

0020-1669/83/1322-1704$01.50/0